J Solid State Electrochem (2006) 10: 689–695
DOI 10.1007/s10008-006-0112-4

ORIGINAL PAPER

J. Flis · M. Kuczynska-Wydorska · I. Flis-Kabulska

The effect of molybdenum on corrosion of low-temperature nitrided stainless steels in sulphate–chloride solution

Received: 9 May 2005 / Accepted: 9 November 2005 / Published online: 5 May 2006

Abstract Resistance of stainless steels to pitting corrosion is strongly enhanced by nitriding at 380–450 °C. In this work, anodic behaviour of steels with 0.13, 2.1, 4.5 and 6.1 wt% Mo was studied before and after nitriding at 450 °C for 30 h which gave 13.0–15.8 wt% N at the surface. Electrochemical measurements were carried out in 0.1 M Na_2SO_4 + 0.4 M NaCl at pH 3.0. Nitriding of steels with lower Mo contents (0.13 and 2.1 wt% Mo) enhanced the resistance to pitting corrosion; steels with higher Mo contents retained their high resistance to pitting but underwent an activation. Nitrogen increased anodic reactivity in initial stages of polarisation, and it also increased the passivation rate. X-ray photoelectron spectroscopy analysis showed that anodic films on nitrided steels contained oxides at the outer surface and Cr–N species deeper from the surface. The enhanced resistance to pitting corrosion of low-temperature nitrided steels is explained by the increased anodic reactivity which leads to the formation of a salt-type film with Cr/Fe oxides and Cr–N species.

Keywords Stainless steels · Nitriding · Corrosion · Surface films

Introduction

Conventional nitriding of stainless steels is performed at temperatures 550–600 °C for the purpose of increasing the yield and fatigue strength, hardness and wear resistance [1–3]. The improvement of mechanical properties results from the precipitation of chromium nitrides which, however, cause a deterioration of corrosion resistance [4–7] due to chromium depletion of the matrix [4] and heterogeneity of the structure.

To avoid the formation of nitride precipitates, nitrogen is introduced into stainless steels at lower temperatures—about 380 to 450 °C. This low-temperature nitriding produces so-called S phase [8], being a supersaturated solid solution of nitrogen [4, 8–13] with up to about 13 wt% N [9]; this phase has the body centered tetragonal (bct) structure [14].

Nitriding at low temperatures results in a considerable improvement of the resistance of stainless steels to pitting corrosion. Higher resistance than that of untreated steels was observed in the neutral [4, 11, 15, 16] and acidified chloride solutions [17, 18]. However, a decreased corrosion resistance of low-temperature nitrided 304L steel was observed in 0.1 M Na_2SO_4 acidified to pH 3.0 [19].

High resistance to pitting of low-temperature nitrided stainless steels is consistent with the beneficial effect of nitrogen on corrosion resistance. The extensive literature on the effect of nitrogen at low concentrations has been reviewed in a book [20] and in publications [21–24]. Most recognised explanations of this effect involve the formation of NH_4^+ with the resultant alkalisation [25, 26] and the segregation of nitrogen under the passive film [27, 28]. Beneficial effect of nitrogen is strongly enhanced by molybdenum; the literature on the effect of molybdenum and on nitrogen–molybdenum synergism is reviewed in [29] and [20, 24], respectively. Molybdenum can act through inhibiting effect of MO_4^{2-} [30–32], by retarding the dissolution due to metallic Mo segregated at the surface [33–35], by the formation of a salt film [36] and by other effects [29]. To explain the nitrogen–molybdenum synergy, Newman and Shahrabi [21] suggested a specific interaction between Mo and N; Lu et al. [37] suggested that the increase in pH due to NH_3 facilitates the formation of molybdates which enhance the passivity. The importance of the increase in pH and the role of interaction between ammonia and molybdates formed from Mo and N is also discussed in [38, 39].

Most of the research on the effect of nitrogen has been performed on steels with N at low concentrations (below

In Honour of Professor Kurt Schwabe.

J. Flis (✉) · M. Kuczynska-Wydorska · I. Flis-Kabulska
Institute of Physical Chemistry of the Polish
Academy of Sciences,
01-224 Warsaw, Poland
e-mail: jflis@ichf.edu.pl
Tel.: +48-22-3433235
Fax: +48-22-6325276

1 wt%), not exceeding the solubility. In the present work, low-temperature nitrided steels with various contents of molybdenum were used to determine the effect of nitrogen at its high concentrations (about 13.0–15.8 wt% N) on corrosion and passivation of austenitic steels.

Materials and methods

Four commercial steels of the types AISI 304L, AISI 316L, AISI 904L and 254 SMO (Avesta Sheffield AB) were used; their composition is given in Table 1. Samples 25×25×3 mm were plasma nitrided in a gas mixture of 80 vol% N_2 + 20 vol% H_2 under pressure of 500 Pa at temperature of 425 °C for 30 h.

Concentration profiles of the elements were determined by glow discharge optical emission spectroscopy (GDOES). Structure of nitrided layers was characterized with x-ray diffraction (XRD), whereas composition of anodic films was examined with x-ray photoelectron spectroscopy (XPS). The latter measurements were carried out with the use of Al Kα radiation at the voltage of 10 kV and current of 10 mA. Depth profiles were obtained by Ar^+ ion sputtering at the voltage of 3.0 kV and the ion gun current of 5 μA cm^{-2}.

Electrochemical measurements were made on unnitrided and nitrided steels, in the latter case on the as-nitrided surface (outer surface without polishing). Measurements were made at ambient temperature in a non-deaerated solution of 0.1 M Na_2SO_4 + 0.4 M NaCl, acidified to pH 3.0 by the addition of H_2SO_4. The measurements were performed in a conical glass vessel in which samples were clamped via a rubber washer to a hole of 6.4 mm diameter at the bottom. The potentials were measured and reported against a mercury sulphate electrode $Hg|Hg_2SO_4|0.1$ M Na_2SO_4 (designated here as MSE) (E^o (MSE)=+0.661 V (NHE)=+0.420 V(SCE)). Polarisation curves were measured at a potential scan rate of 1 mV s^{-1} after a 2-min hold at an initial potential of −1.4 V(MSE) to standardize the surface conditions.

In potentiostatic measurements, anodic potentials were applied after holding under the open-circuit conditions for about 3 min. Fast current decay transients were recorded at times from 10^{-5} s up to 3 h after applying the potential.

Table 1 Chemical composition (wt%) of stainless steels used in this work (Fe balance)

Steel	C	Cr	Ni	Mo	Mn	Cu	N
AISI 304L	0.02	18.1	9.0	0.13	1.54	0.22	0.05
AISI 316L	0.02	16.9	11.2	2.1	1.47	0.03	0.06
AISI 904L	0.01	20.0	25.0	4.5	1.43	1.50	0.06
254 SMO	0.02	20.0	18.0	6.1	0.68	0.73	0.20

Results

Composition and structure

GDOES analysis indicated that the as-nitrided surfaces contained 13.0 wt% N in 304L and 316L steels and 15.8 wt% N in 904L and 254 SMO steels; nitrogen entered to the depths of 14–16 μm. Concentration profiles of nitrogen and chromium in nitrided 304L and 316L steels (Fig. 1) show that down to the depths of about 1–2 μm, the concentrations of these elements decreased in a similar way; this suggests that Cr and N were bound with each other.

XRD patterns of unnitrided and nitrided 304L steel are shown in Fig. 2. Peaks S1 and S2 for nitrided steel, occurring at lower angles than the γ(111) and γ(200) peaks for the austenitic matrix, indicate an expanded austenite. They show the presence of a nitrogen supersaturated solid solution (S phase), which was earlier observed by other authors [4, 8–13]. The diffraction pattern did not reveal second phases.

Electrochemical measurements

Anodic polarisation curves

Anodic polarisation curves for unnitrided and nitrided steels in the solution used are shown in Fig. 3. For unnitrided 304L steel, a steep rise of current occurred in the passive region, demonstrating the growth of stable pits. The potential of the start of the current rise is designated by E_p (pitting potential). Oscillations of current below E_p are characteristic for metastable pitting [20]. For nitrided steel, pitting potential E_p occurred at a much nobler potential, manifesting higher resistance to the localized corrosion. Still higher resistance was exhibited by nitrided 316L steel (not shown here)—this steel did not undergo pitting corrosion in the entire potential range.

In contrast to 304L and 316L steels, nitrided 904L and 254 SMO steels became less resistant to chloride anions. Owing to high molybdenum contents, the untreated steels possess very high resistance to pitting and crevice corrosion, especially in acids with chlorides. In accordance, polarisation curves (Fig. 3) show that untreated 904L and 254 SMO steels were resistant to pitting in the entire potential range. However, nitrided steels did not retain passivity in the chloride solution. Polarisation curves show a region of the active dissolution, then the occurrence of a passivation and next a rise of current. The current rise denotes an activation; therefore, the potential of the start of this rise is designated as the activation potential (E_{act}). In case of 254 SMO steel, slight oscillations of current occurred, suggesting the formation of metastable pits. However, the increased current above E_{act} was not associated with typical pitting. Surface of the samples

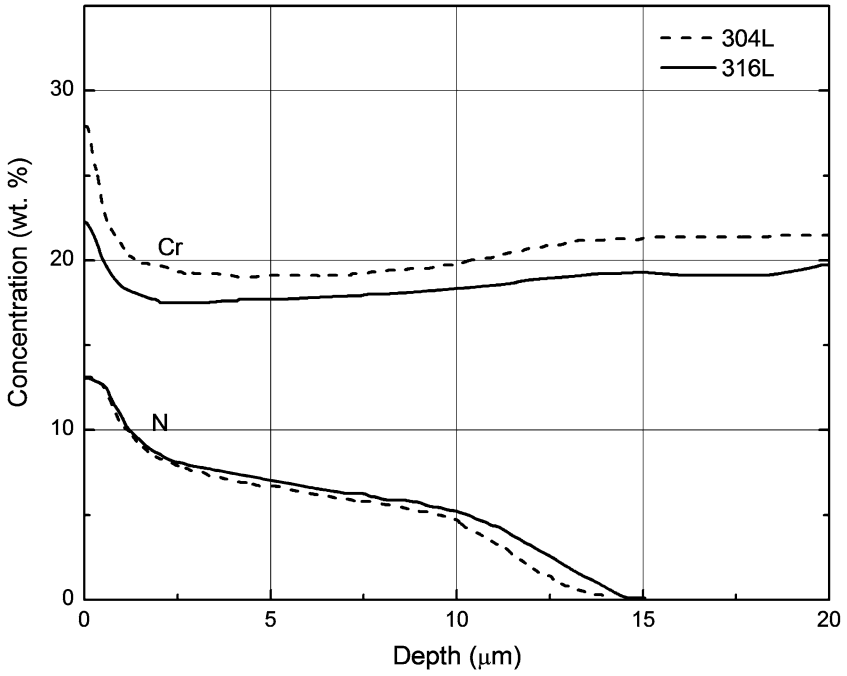

Fig. 1 Glow discharge optical emission spectroscopy concentration profiles of nitrogen and chromium in 304L and 316L steels nitrided at 425 °C for 30 h

after the polarisation measurements was rough, occasionally with small shallow cavities, but free of regular pits.

For all the steels, anodic currents after nitriding were higher than those for unnitrided steels (disregarding currents above E_p for unnitrided 304L and 316 steels). This may suggest that the high resistance to pitting of low-temperature nitrided steels might be in some way associated with their increased anodic reactivity. In order to find out whether this can be possible, current transients were measured under potentiostatic conditions.

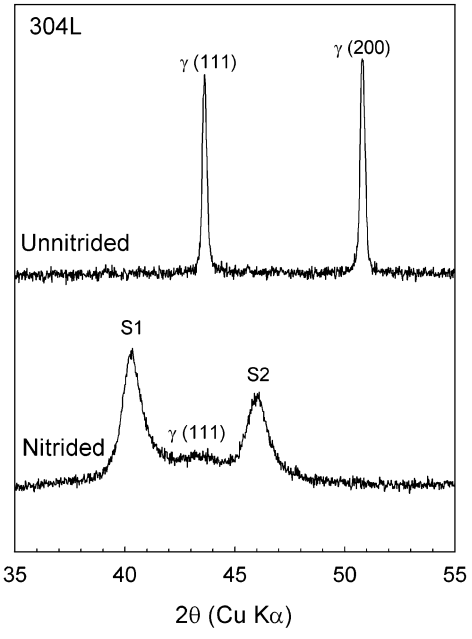

Fig. 2 X-ray diffraction patterns of 304L steel unnitrided and nitrided at 425 °C for 30 h

Potentiostatic measurements

The measurements were carried out at potentials by 0.1 V more negative than the pitting potentials E_p for unnitrided 304L and 316L steels, or the activation potentials E_{act} for nitrided 904L and 254 SMO steels (Fig. 3). Currents were recorded at times from 10^{-5} s after applying these potentials, but it should be borne in mind that the currents at the shortest times (about 10^{-5} s) can be affected by various instrumental artifacts; hence, they may not be purely faradaic. Nevertheless, current transients shown in Fig. 4 include also the shortest times. The rise of the current for unnitrided 304L and 316L steels after about 100 and 2000 s, respectively, was associated with the growth of stable pits. Apart from that, the currents for nitrided steels were much higher than those for unnitrided steels.

In the initial period up to about 0.5 to 10 s, three steps can be distinguished, as marked in Fig. 4 on the curve for nitrided 304L steel. These steps appear on all the curves except the curve for unnitrided 254 SMO steel, which does not exhibit step 2. Step 1 has the highest current and is the shortest; probably, it is associated with anodic oxidation of the metal. Step 2 is for nitrided steels significantly larger than for unnitrided steels. Possibly, at this step, there occurred oxidation of corrosion products which were formed at step 1; hence, larger step 2 may indicate larger amount of corrosion products.

Step 3 denotes the occurrence of passivation. The $\Delta \log I / \Delta \log t$ slopes of the fast current decay were for nitrided steels steeper than those for unnitrided steels. For unnitrided and nitrided 304L steel, the slopes were −1.0 and −1.3, respectively, and for 316L steel, they were −0.81 and −1.7, respectively. Slope of −1.0 characterizes oxide film growth through high field or direct logarithmic kinetics [40]. Slopes steeper than −1 are usually ascribed

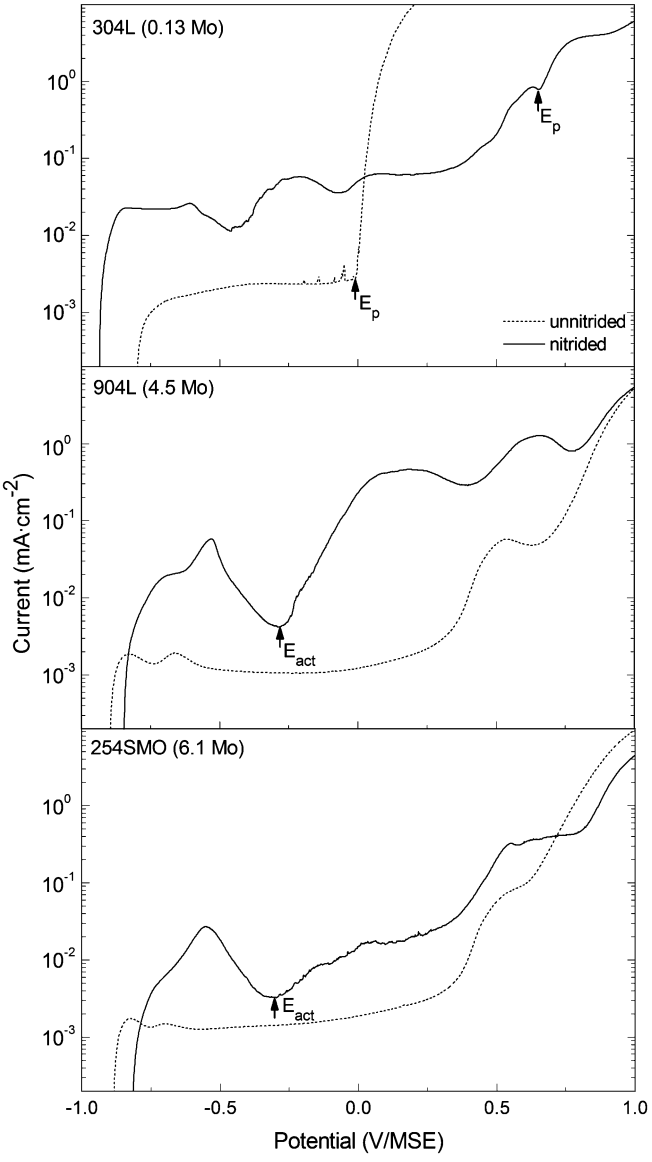

Fig. 3 Polarisation curves for unnitrided and nitrided steels 304L, 904L and 254 SMO in 0.1 M Na_2SO_4 + 0.4 M NaCl, pH 3.0. E_p and E_{act} are pitting and activation potentials, respectively

to the precipitation of salts; therefore, the increased slopes for nitrided steels suggest precipitation of salt films.

These measurements indicate that nitrogen in a solid solution in austenite increases the initial active anodic oxidation of the steels, and it also increases the rate of the subsequent passivation.

Atomic force microscopy examination

Figure 5 shows the surfaces of unnitrided and nitrided 304L steel after polarisation at −0.11 V (MSE) for 100 s and after subsequent removal of corrosion products by Ar^+ ion sputtering. In accordance with the electrochemical results, pits occurred on unnitrided steel on the surface which otherwise remained unattacked. Evidently, pits grew on the passivated surface. On the contrary, nitrided steel was strongly corroded; its surface was rough, but it did not exhibit typical pits.

Analysis of surface films

XPS analysis of surface films was carried out after polarisation for 100 s at the potentials of the potentiostatic measurements (Fig. 4). Atomic concentration–depth profiles for unnitrided and nitrided 304L and 316L steels are shown in Fig. 6. Characteristic features of these profiles are as follows:

1. Films on unnitrided steels contained large amounts of oxygen; at the maximum on the O profile, there occurred a small maximum on the Cr profile and a slight shoulder on the Fe profile. This indicates that the films on unnitrided steels were composed mainly of the Cr and Fe oxides.
2. Films on nitrided steels contained much less oxygen compared with unnitrided steels. In addition, they contained nitrogen.
3. On nitrided steels, distribution of O, Cr, Fe and N in films was similar for both steels. At the outer surface, maxima of oxygen O appeared which coincided with small steps on the Cr and Fe profiles. This demonstrated the presence of Cr and Fe oxides (and/or oxyhydroxides); however, their content was definitely smaller than that on unnitrided steels. Deeper from the surface, wide maxima of Cr and N occurred. Profiles of these two elements were similar; therefore, it can be suggested that these elements were bound with each other to form species which are designated here as Cr–N species. At the surface of 316L steel, a small maximum on Mo profile coincided with the O maximum; the Mo–O species are probably molybdates. These concentration–depth profiles indicate that anodic films on nitrided steels contained predominantly Cr and Fe oxides (and/or oxyhydroxides) near the surface and Cr–N species deeper from the surface. Films on 316L steel can also contain molybdates (Mo–O species).
4. Outer layers of the films on nitrided steels did not contain Ni compounds.

Discussion

Low-temperature nitriding resulted in a significant increase of the resistance to pitting corrosion of austenitic steels 304L and 316L, having rather low contents of Mo (0.13 and 2.1 wt% Mo, respectively), but it increased anodic reactivity in the passive region of 904L and 254 SMO with higher Mo contents (4.5 and 6.1 wt% Mo, respectively).

It is suggested that these effects are associated with the increased anodic reactivity of nitrided steels. This is demonstrated by an increased anodic current at potentials below E_p or E_{act} (Fig. 3) and an increased current during

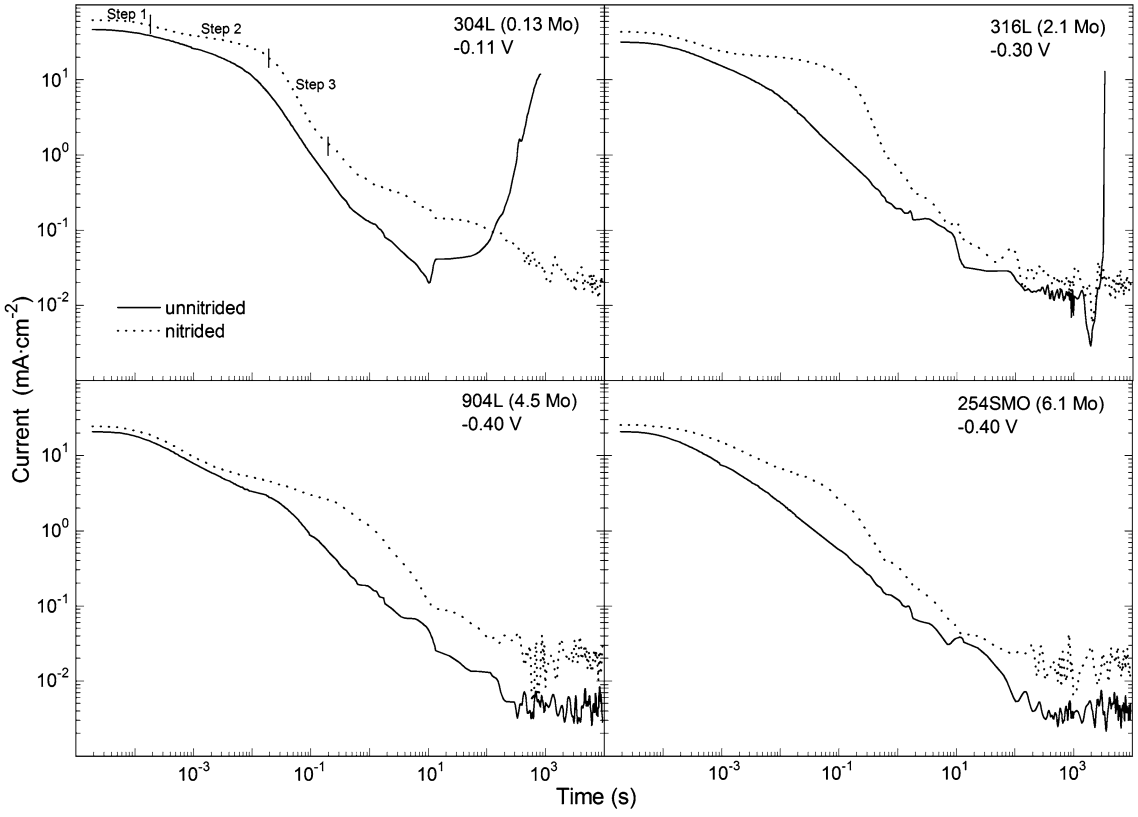

Fig. 4 Current transients for unnitrided and nitrided steels in 0.1 M Na_2SO_4 + 0.4 M NaCl, pH 3.0, at given potentials which are by −0.1 V below E_p (pitting potential for unnitrided 304L and 316L steels) or below E_{act} (activation potential for nitrided 904L and 254 SMO steels). Steps 1–3 denote distinct stages of current transients

potentiostatic measurements (Fig. 4). In the latter case, step 2 can be due to anodic oxidation of corrosion products formed at step 1. Judging from the potentials of electrochemical equilibria [41], at the potentials shown in Fig. 4, the following reactions can take place at step 2:

1. Fe(II)→Fe(III)
2. Cr(II)→Cr(III)
3. Mo(II)→Mo(IV) and Mo(VI) (molybdates MoO_4^{2-})

All these oxidation products can exert a passivating effect. This effect is demonstrated by steeper $\Delta \log I / \Delta \log t$ slopes at step 3. Slopes above −1 suggest the passivation by the precipitation mechanism; hence, steeper slopes for nitrided steels may indicate a contribution of the salt precipitation to the faster passivation.

The steepest slope occurred for 316L with 2.1 wt% Mo, probably owing to the formation of molybdates which are effective corrosion inhibitors, in particular of pitting corrosion in chloride solutions [20, 32].

If passivation rate is affected by corrosion products, faster passivation of nitrided steels can be associated with faster accumulation of corrosion products exerting an inhibitive effect [Fe(III), Cr(III), molybdates]. Therefore, more effective inhibition would be a consequence of a faster initial anodic dissolution of nitrided steels. An increased anodic reactivity of low-temperature nitrided 304L steel was also observed in other works [18, 19, 42]; it

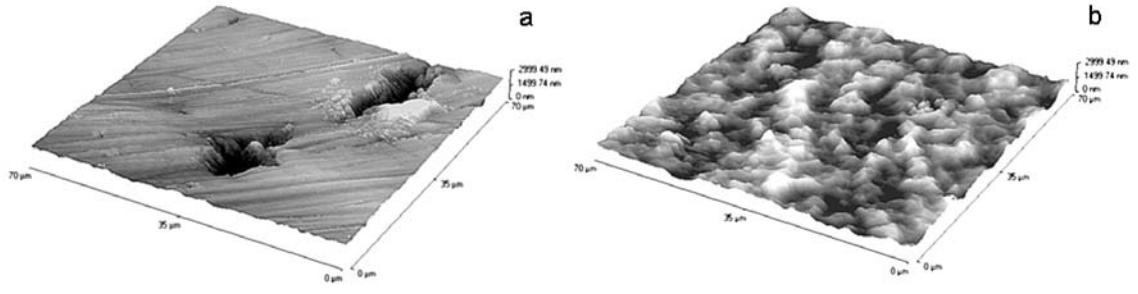

Fig. 5 Atomic force microscopy images of unnitrided (**a**) and nitrided (**b**) 304L steel after polarisation in 0.1 M Na_2SO_4 + 0.4 M NaCl, pH 3.0, at −0.11 V (mercury sulphate electrode) for 100 s (current transients are shown in Fig. 4) and subsequent removal of corrosion products by Ar^+ ion sputtering. Pits occur only on unnitrided steel

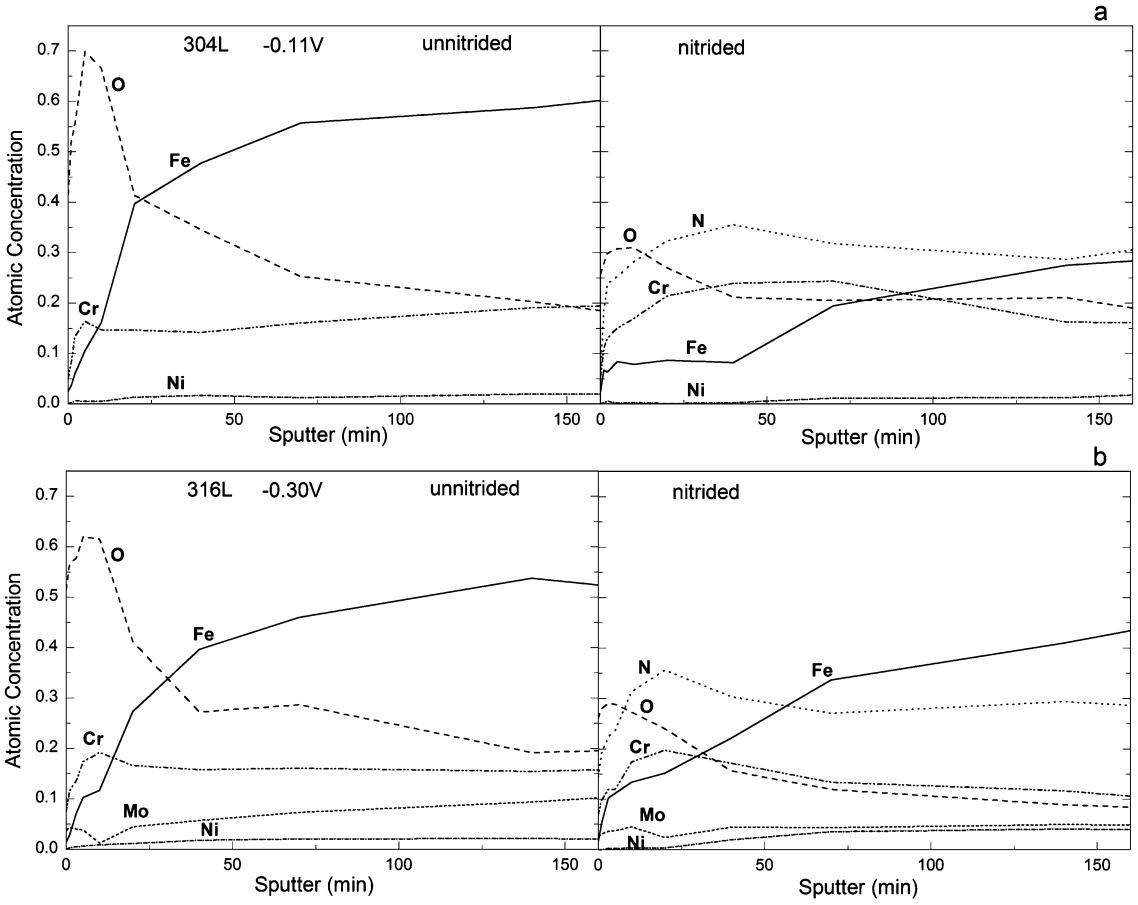

Fig. 6 X-ray photoelectron spectroscopy concentration–depth profiles for unnitrided and nitrided 304L and 316L steels after a 100-s polarisation in 0.1 M Na_2SO_4 + 0.4 M NaCl, pH 3.0, at potentials as in Fig. 4

can be due to lower thermodynamic stability of the supersaturated solid solution of nitrogen in austenite and/or to a possible presence of some chromium nitride precipitates in this solution. The XRD pattern (Fig. 2) did not reveal second phases; nevertheless, some small precipitates cannot be excluded due to a possible decomposition of S phase [43].

Anodic films on nitrided steels strongly differ from those on unnitrided steels. Concentration profiles (Fig. 6) show that the films on unnitrided steels were composed of oxides, whereas the films on nitrided steels were a mixture of oxides and/or oxyhydroxides (predominantly at the outer surface) and of Cr–N species (predominantly in deeper layers); they can also contain salts (molybdates, sulphates, chlorides). Salt films are less protective than passivating oxide films, but they are less vulnerable to a breakdown by chloride anions.

Cr–N species might strongly contribute to the protection against pitting. Their nature cannot be unequivocally recognised. It was shown [18] that electron binding energies of nitrogen-containing species corresponded to chromium nitrides; however, nitrides are not expected in low-temperature nitrided steels, and they have not been revealed by XRD (Fig. 2) [18]. Maybe these are some species of the S phase, and also it is possible that these are tiny precipitates of CrN nitride which were formed due to some decomposition of the solid nitrogen solution despite of the low temperature. Chromium nitride CrN is resistant to anodic oxidation [44]; hence, its presence in anodic films can provide a protective effect.

It is proposed that the high resistance to pitting corrosion of low-temperature nitrided stainless steels can be explained as follows:

- *Primary effect*: increased anodic reactivity.
- Due to the presence of nitrogen (dissolved in austenite lattice and/or in tiny nitride precipitates), anodic oxidation rate is increased.
- *Secondary effect*: due to the accelerated anodic dissolution, larger amounts of corrosion products and of Cr–N species accumulate on the surface. This results in:
- formation of a salt film instead of an oxide film
- incorporation of larger amounts of Cr and Fe oxides and/or oxyhydroxides (passivating species), molybdates in case of Mo-containing steels (inhibiting species) and of Cr–N species (corrosion-resistant material)

Cr–N species were present within a fairly large depth range (Fig. 6); hence, in this case, the explanation based on the segregation of nitrogen under the passive film [27, 28] cannot be applied. The suggestion on the formation of

molybdates on Mo-containing steels is in agreement with works by Ogawa et al. and Ilevbara and Burstein [30–32].

This work does not provide a direct evidence for the N–Mo synergy; nevertheless, it shows that the presence of nitrogen in the Mo-containing steel leads to an accelerated passivation and to an increased content of Mo–O compounds, probably molybdates, in corrosion products in the acidic solution. Also, Eckstein et al. [45, 46] found that passivating effect of nitrogen increases strongly with the increasing content of Mo in stainless steels in an acidic electrolyte HCl + NaCl (pH 1.3); however, these authors did not observe any effect of Mo on effectiveness of nitrogen on pitting corrosion in neutral NaCl solutions (pH 5.9). It can be suggested that the lack of the N–Mo synergy in neutral solutions, reported in [45, 46], might be due to insufficient dissolution of the Mo-containing steel.

Conclusions

Effect of high concentrations of nitrogen in austenitic stainless steels on anodic behaviour was examined on 304L, 316L, 904L and 254 SMO steels with 0.13, 2.1, 4.5 and 6.1 wt% Mo, respectively. Nitrogen was introduced by plasma nitriding at 450 °C for 30 h. Electrochemical measurements were performed in a sulphate–chloride solution of pH 3 on outer surfaces which contained 13.0–15.8 wt% N. Conclusions are as follows.

Nitrogen increased the resistance to pitting corrosion of steels with 0.13 and 2.1 wt% Mo, but it increased anodic dissolution in the passive region of steels with 4.5 and 6.1 wt% Mo.

Nitrogen increased anodic reactivity in the initial stages of polarisation, and it also increased the rate of the subsequent passivation.

Anodic films on unnitrided steels were composed of oxides, whereas the films on nitrided steels contained small amount of oxides at the outer surface, and additionally Cr–N species deeper from the surface.

It is proposed that the enhanced resistance to pitting corrosion of low-temperature nitrided steels results from their increased anodic reactivity which leads to the formation of a salt-type film with Cr/Fe oxides and with Cr–N species. The latter can be corrosion resistant similarly as CrN.

References

1. Rayaprolu DB, Hendry A (1988) Materials Sci Technol 4:136
2. Datta FK, Gray JS (eds) (1993) Surface engineering. Royal Society of Chemistry, Cambridge
3. Spalvins T, Kovacs WL (eds) (1990) Ion nitriding and ion carburizing. ASM International, Materials Park, OH
4. Zhang ZI, Bell T (1985) Surf Eng 1:131
5. Flis J, Mankowski J, Rolinski E (1989) Surf Eng 5:151
6. Flis J, Mankowski J, Zakroczymski T (2000) Corros Sci 42:313
7. Bandy R, Van Rooyen R (1985) Corrosion 41:228
8. Ichii K, Fujimura K, Takase T (1986) Technol Rep Kansai Univ 27:135
9. Gemma K, Kawakami M (1989) High Temp Mater Process 8:205
10. Samandi M, Shedden BA, Bell T, Collins GA, Hutchings R, Tendys J (1994) J Vac Sci Technol B 12:935
11. Menthe E, Rie K-T, Schultze JW, Simson S (1995) Surf Coat Technol 74–75:412
12. Sun Y, Li XY, Bell T (1999) J Mater Sci 34:4793
13. Larisch B, Brusky U, Spies HJ (1999) Surf Coat Technol 119:205
14. Angelini E, Burdese A, DeBenedetti B (1988) Metall Sci Technol 6:33
15. Dearnley PA, Namvar A, Hibberd GGA, Bell T (1989) In: Broszeit E, Munz WD, Oechsner H, Rie K-T, Wolf GK (eds) Plasma surface engineering, vol 1. DGM Informationsgesellschaft, Oberursel, p 219
16. Sun Y, Bell T, Kolosvary Z, Flis J (1999) Heat Treat Met 26:9
17. Lei MK, Zhu XM (2001) Biomaterials 22:641
18. Flis J, Kuczynska M (2004) J Electrochem Soc 151:B573
19. Flis J, Gajek A (2001) J Electroanal Chem 515:82
20. Szklarska-Smialowska Z (2005) Pitting and crevice corrosion. NACE, Houston, TX
21. Newman RC, Shahrabi T (1987) Corros Sci 27:827
22. Levey PR, van Bennekom A (1995) Corrosion 51:911
23. Grabke HJ (1996) ISIJ Int 36:777
24. Jargelius-Pettersson RFA (1999) Corros Sci 41:1639
25. Osozawa K, Okato N (1976) In: Proc. USA–Japan seminar: passivity and its breakdown on iron and iron-based alloys. NACE, Honolulu pp 135–139
26. Baba H, Kodama T, Katada Y (2002) Corros Sci 44:2393
27. Lu YC, Bandy R, Clayton CR, Newman RC (1983) J Electrochem Soc 130:1774
28. Ahila S, Reynders B, Grabke HJ (1996) Corros Sci 38:1991
29. Jargelius-Pettersson RFA, Pound BG (1998) J Electrochem Soc 145:1462
30. Ogawa H, Omata H, Itoh I, Okdada H (1978) Corrosion 34:52
31. Ilevbara GO, Burstein GT (2001) Corros Sci 43:485
32. Ilevbara GO, Burstein GT (2001) Corros Sci 45:1545
33. Olefjord I (1980) Mater Sci Eng 42:161
34. Newman RC (1985) Corros Sci 25:331
35. Burstein GT (1985) Proc UK Corrosion '1985, p 84
36. Newman RC, Betts AJ (1987) In: Advances in localized corrosion. NACE-9, Houston, TX p 271
37. Lu YC, Ives MB, Clayton CR (1993) Corros Sci 35:89
38. Olsson C-O (1995) Corros Sci 37:467
39. Olefjord I, Wegrelius L (1996) Corros Sci 38:1203
40. Burstein GT, Davenport AJ (1989) J Electrochem Soc 136:936
41. Pourbaix M (1966) Atlas of electrochemical equilibria in aqueous solutions. Pergamon, Oxford
42. Flis J, Kuczynska M (2003) Mater Corros 54:953
43. Li XY (2001) Surf Engin 17:147
44. Ibrahim MAM, Korablov SF, Yoshimura M (2002) Corros Sci 44:815
45. Eckstein Ch, Spies H-J, Zimdars H (2003) Mater Corros 54:176
46. Eckstein Ch, Spies H-J, Albrecht J (2004) Mater Corros 55:861